The mass stiffness of residual dolomite from large surcharge trials

S. W. Jacobsz

Department of Civil Engineering, University of Pretoria, University Avenue, Pretoria, Gauteng 0002, South Africa
(e-mail: sw.jacobsz@up.ac.za)

Abstract: In South Africa, the stiffness of dolomite residuum has traditionally been viewed as relatively low. For reasons of economy, available dolomite residuum stiffness data mostly stem from plate load tests on each of the materials forming the residual profile, typically chert gravels and wad, rather than on the actual mix of materials that typically occurs *in situ*. This paper presents back-calculated stiffness values from a series of large-scale surcharge trials carried out in Centurion, south of Pretoria, for the Gautrain Rapid Rail Project. It is shown that the mass stiffness of the residual dolomite profile is significantly higher than the traditionally recognized values of its constituents, allowing the viaducts for the Gautrain south of Pretoria to be founded on dolomite residuum instead of bedrock.

In the Centurion area south of Pretoria, the Gautrain railway line, linking the cities of Pretoria and Johannesburg, crosses the Malmani dolomites of the Transvaal Supergroup (see, e.g. Johnson et al. 2006). It was decided to construct the Centurion section on a *c*. 3 km long viaduct supported on about 70 piers, generally spaced 44 m apart. The pier heights vary, but are approximately 12 m. A typical pier dead load is *c*. 30000 kN. The contractor was faced with the problem of constructing the viaduct foundation on or in a dolomitic profile and proposed at tender stage to found the viaduct piers on groups of large diameter (1.5 m) piles end-bearing on dolomite bedrock. Owing to the difficulties associated with constructing piles end-bearing on the highly irregular dolomite bedrock surface, other foundation solutions, avoiding piling to rock, were considered. This meant that foundations had to be founded in or on the residual or transported materials above bedrock, which traditionally had been assumed to be highly compressible and prone to the formation of sinkholes.

A series of large-scale surcharge trials, designed to quantify the mass stiffness of the soil profile above bedrock, were carried out. The surcharge trials, observed settlements, analysis of results and the back-calculated stiffness values are presented in this paper.

Geology and ground profile

South of Pretoria, travelling in a northerly direction, the Gautrain track alignment crosses respectively the Oaktree, Monté Christo, Lyttleton and Eccles formations of the Malmani Subgroup of dolomites of the Transvaal Basin. The dolomites have ages of *c*. 2500 Ma (Johnson et al. 2006) and have, as a consequence, weathered dramatically along joint planes, leaving a karst bedrock topography with deep gullies or trenches, flanked by dolomite rock pinnacles. The dolomite bedrock is typically interbedded with chert, shale and quartzite, the quantities of which vary between the various formations. The gullies in the bedrock are often filled with unconsolidated weathering products comprising chert fragments from sand to boulder sizes and highly variable proportions of manganiferous earth (wad), which is highly erodible. The weathering products can also occur as an overburden above the rock head. Cavities, ranging from very small up to several metres in diameter, can occur.

The residual materials above bedrock usually comprise chert gravels and boulders in a matrix of clayey and silty sands. The residual profile is usually overlain by colluvial deposits ranging in thickness up to about 10 m. Materials generally tend to become more porous and more compressible with depth.

Figure 1 presents two photographs of dolomite bedrock exposed at the Lyttelton quarry in Centurion. It shows a large number of rock pinnacles, apparently randomly distributed, giving an extremely variable rock head surface with steep subvertical slopes. These rock head conditions are likely to be representative of the conditions occurring underneath much of the Centurion viaducts. The situation is further illustrated by a summarized borehole record from viaduct Pier 45 in Figure 2. It presents the soil profiles determined from four percussion boreholes drilled on the centrelines of the proposed pile positions at this pier. It illustrates extreme variability in depth to bedrock over short distances, as well as the presence of large cavities in the rock.

The degree of weathering of the intact dolomite bedrock tends to be minimal. The rock is typically extremely hard and exhibits uniaxial compressive strengths of well above 300 MPa (see, e.g. Wagener 1982).

A major problem associated with the dolomites is the sudden appearance of potentially large sinkholes (sometime tens of metres in diameter) owing to near-surface residual and transported materials eroding into solution cavities in the bedrock. This is especially associated with leaking pipes and water ingress into the ground and is exacerbated by the lowering of the ground water table.

The overall geological profile can be described as extremely heterogeneous in terms of composition, depth to bedrock and engineering properties. The profile is, as a consequence, extremely difficult to characterize for foundation design purposes.

In summary, the ground profile along the viaduct comprised chert gravels and boulders in a matrix of hillwash sand, underlain by a potentially compressible and voided dolomite residuum comprising wad with minor chert (according to borehole logs from the site investigation (Bombela CJV 2007)). An important characteristic of the soil profile is its extreme heterogeneity, as it typically contains numerous chert fragments, ranging from gravels to large boulders in a matrix comprising any material from clay, ranging through silty sands, to gravels and boulders.

Fig. 1. Dolomite pinnacles exposed in the Lyttelton area.

Difficulties associated with ground investigations

For the design of a founding solution, the bedrock profile and thickness of the underlying competent rock have to be defined in some detail. This is less problematic in horizontally or subhorizontally bedded profiles, but in the profile described, no economical number of boreholes would allow the bedrock profile to be characterized in sufficient detail to allow a foundation, bearing on bedrock, to be detailed with confidence. Numerous cavities occur in the dolomite bedrock and uncertainty regarding their detection is unavoidable. By means of drilling, only the vertical dimension of a cavity can, at best, be defined. As its lateral extent cannot be defined without drilling numerous boreholes, it is not possible to determine with certainty whether the cavity could be grouted or not. Given the heterogeneity of the dolomite profile, proving an adequate thickness of bedrock below the bases of the proposed piles would have necessitated drilling an investigation hole at every pile position.

The initial ground investigation comprised the drilling of percussion boreholes along the axis of every proposed large diameter pile forming part of the pile groups supporting the viaduct piers. A considerable effort went into the investigation of additional means by which the foundation conditions could be characterized in greater detail. Trials were carried out using various geophysical methods, including borehole radar (see Tosen et al. 2009), but the variability of the bedrock profile was simply too great to be defined in sufficient detail by such methods.

The only way to completely define a bedrock profile in a situation as illustrated in Figure 1 is to expose it, which was not feasible given the thickness of overburden and the number of viaduct piers to construct. (Exposure of the foundation by sinking shaft foundations was selected for some piers, but could not be used at all piers because of the high cost.)

A further complication associated with founding the viaduct on dolomitic bedrock was that, should unsuitable founding conditions (e.g. a large cavern underneath a thin rock cover or excessive depth to competent bedrock) be encountered, it might not have been possible to move the pier in question to suitable founding conditions within the constraints imposed by the viaduct geometry.

This situation led to the conclusion that rock head conditions could not be defined at reasonable cost in sufficient detail to allow pile construction to proceed without considerable risk. A bedrock profile as illustrated in Figure 1, in combination with the fact that the dolomite rock is extremely hard, typically results in serious difficulties during pile installation. Problems are usually revealed only during construction and then have to be dealt with at construction, which is why experienced local geotechnical contractors are hesitant to pile in the dolomites. Thus, consideration of alternative founding solutions was required. Heavy structures such as silos have in the past been founded on residual dolomitic profiles where the foundations did not extend to bedrock (Wagener 1982; Day, pers. comm.). This option was also considered for the Gautrain Viaducts in Centurion. An important issue associated with such a founding solution is the potential settlement of the foundation if placed on the residual soil, and it was therefore necessary to characterize the mass stiffness of the residual dolomite profile.

Existing data on the stiffness of residual dolomite

A considerable amount of work has been done on the development on dolomitic land since the 1970s (e.g. Wagener 1982; Buttrick 1986). An important aspect in planning construction on residual dolomite is the stiffness of the residual dolomite profile. The bulk of available knowledge regarding the stiffness of residual dolomite profiles stems from plate load tests on the various materials it comprises. However, because of the fact that necessarily small-diameter plate load tests measure stiffness over only a limited depth and typically at relatively large strains, data from such tests are unlikely to be representative of the mass stiffness of the profile as a whole. Typical Young's moduli from plate load tests for chert gravels and wad are presented in Table 1. These values are presented for comparison with the stiffness values that are representative of the overall soil profile later in the paper.

Large-scale surcharge trials

To assess the mass stiffness of the residual dolomite profile above the dolomite bedrock in response to a typical pier foundation load, a series of large-scale surcharge trials was designed. A typical foundation load would act over an area measuring *c*. 12 m × 12 m. The *in situ* mass stiffness of the residual dolomite profile was measured at various locations along the viaduct alignment by loading a similarly large area to average stresses typical of the actual viaduct.

Ward et al. (1968) reported on a similar large-scale surcharge trial where a large cylindrical water-filled tank, measuring 18.3 m in diameter by 18.3 m high, was used to exert a bearing stress of *c*. 180 kPa on a chalk foundation in the UK. The test set-up was carefully instrumented to measure surface and subsurface movements in response to the filling of the tank. Closed-form elastic solutions, normally used for the calculation of the Young's modulus from plate load tests, were used to back-calculate soil stiffnesses at various depths below the tank.

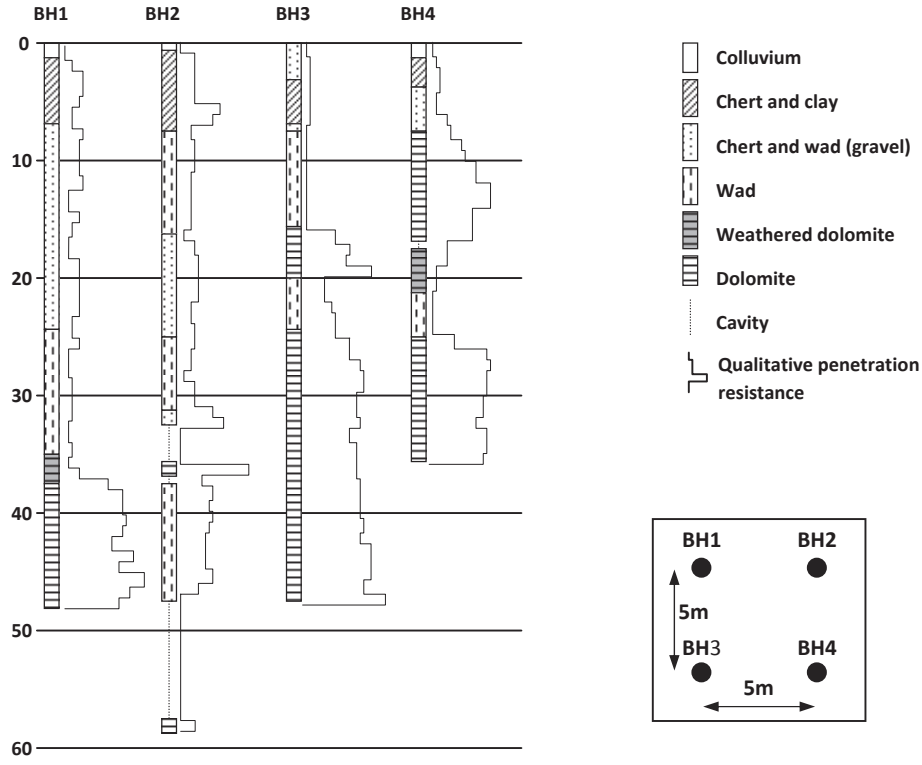

Fig. 2. Borehole profile records from Pier 45 (Bombela CJV 2007).

Table 1. *Typical Young's moduli for dolomitic residuum from vertical plate load tests (data from Wagener 1982)*

Material	Plate modulus (MPa)			Number of samples
	Minimum	Maximum	Average	
Chert gravel	46	109	80	11
Wad	12	22	18	3

Data from Doringkloof, Centurion. Plate diameter is 1 m.

For the Gautrain project, a surcharge arrangement was required that could be moved relatively easily to many pier locations. The surcharge trials comprised the loading of an area measuring *c*. 20 m × 20 m as illustrated diagrammatically in Figure 3. The footprint area of the surcharge was chosen to be larger than the anticipated viaduct pier foundation footprint to ensure than the surcharge would result in effective preloading of all the material at depth within the zone of influence of the foundation. A photograph of the first surcharge trial is presented in Figure 4. The surcharge consisted of 2 m × 2 m × 1 m high concrete blocks, weighing *c*. 9.6 tons each, stacked to a height of between 8 and 10 m, exerting a vertical stress of up to 240 kPa. The blocks were initially placed in four quadrants, separated by 800 mm wide passages to allow access between the blocks for monitoring purposes. Precise levelling benchmarks were installed at various locations around the surcharge to measure surface settlement (see Fig. 3). The settlement monitoring points were constructed by augering 200 mm diameter holes to 1 m and placing 700 mm of concrete into which round-headed bolts were inserted as the measuring points. Precast manhole rings were stacked 300 mm high around each monitoring point to the surface and the ground around each monitoring point was raised somewhat to prevent accumulation of water.

In addition to surface monitoring points, two sets of rod extensometers were installed at the first two surcharge test sites to measure subsurface movements. Because of cost constraints these extensometers were not installed at subsequent test locations.

A concern arose during the stacking of the first surcharge that the surface settlement monitoring points might not accurately reflect the settlement of the concrete blocks themselves owing to the blocks apparently 'sinking' into the ground. The first layer of the surcharge was subsequently modified by stacking the blocks together, removing the access passage at ground level. This was done for all surcharge trials except the first two. Settlement monitoring points were henceforth placed at the same plan locations as before, but bolted to the first layer of blocks so that block settlements and not soil settlements were measured.

Settlements were monitored at four categories of locations. These are the four corners, four at the centre on the inside corners of each quadrant, four at mid-side and four at mid-passage positions (i.e. halfway between the centre and the mid-side positions). The modified surcharge layout is presented in Figure 3b.

The monitoring points were surveyed by means of precise levelling, generally on a daily basis before and during the stacking of the surcharge. The monitoring frequency was reduced once movements had stabilized.

In addition to serving as a monitoring tool for the determination of the *in situ* stiffness of the soil profile, the trials also provided a surcharge acting as pre-loading, so that a higher (reload) stiffness would be expected during subsequent foundation loading.

The surcharge trials were carried out at a total of 30 pier locations along the alignment of the Centurion viaduct.

Calculation of profile stiffness from surcharge settlement

In addition to soil stiffness, the settlement of the surcharge at ground level is affected by several other factors. These include: (1) lateral non-homogeneity of the residual dolomite soil and

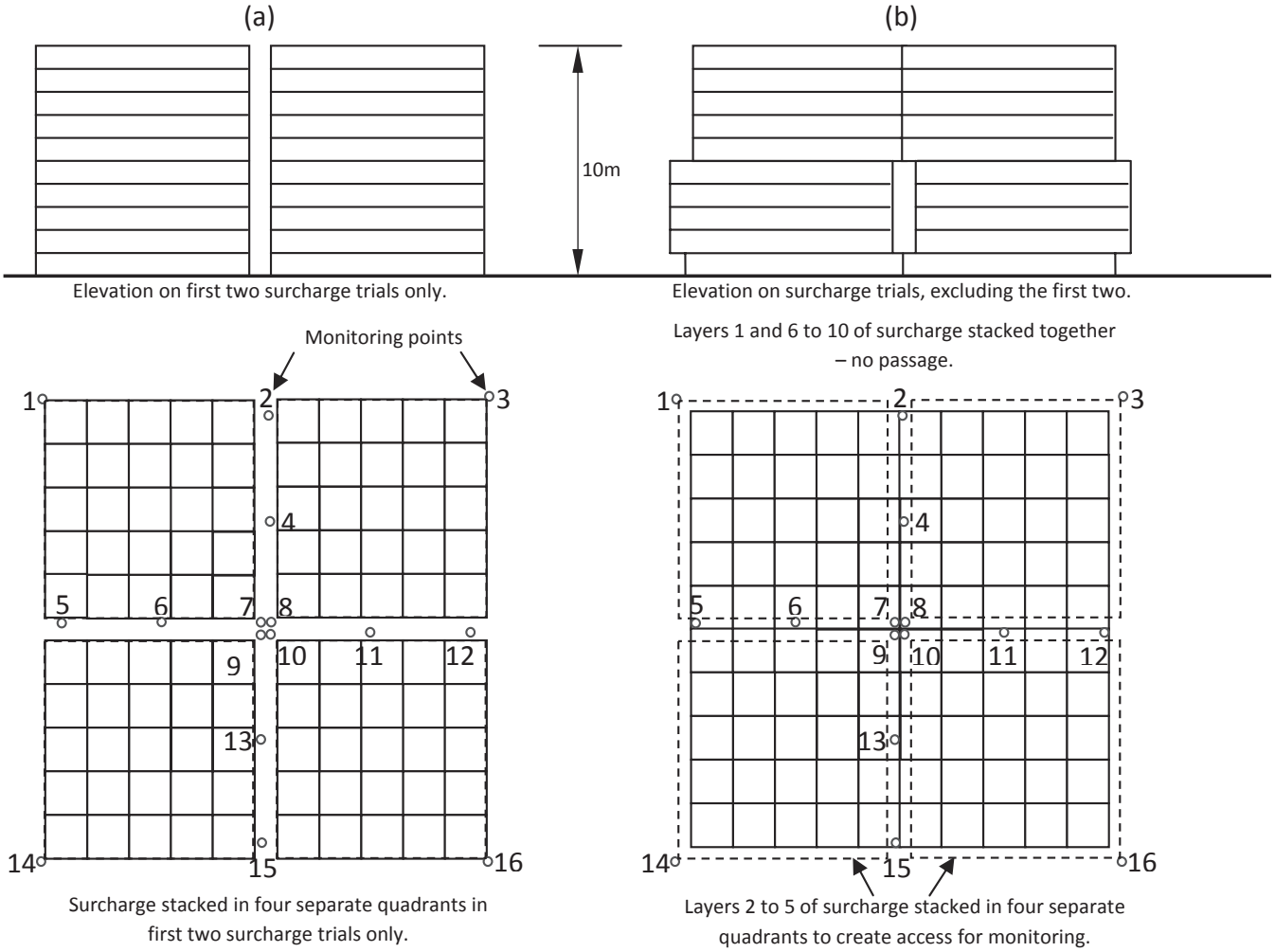

Fig. 3. Elevation and plan views of the two surcharge trial arrangements used.

Fig. 4. The first surcharge stack shortly after completion.

bedrock profiles as illustrated in Figures 1 and 2; (2) non-homogeneity owing to stiffness changes with depth (see, e.g. Gibson 1967, 1974; Rodrigues 1975; Carrier & Christian 1973); (3) stiffness anisotropy (Rodrigues 1975); (4) the non-linearity in stiffness (see, e.g. Jardine et al. 1986); (5) yielding of the soil in response to the load; (6) the degree of rigidity of the loaded area (see, e.g. Gibson 1974; Boswell & Scott 1975), etc.

When back-calculating stiffness moduli, most of these factors can be accounted for using a sufficiently sophisticated numerical model, provided the spatial variability of the ground is known or can be reasonably assumed. However, owing to the uncertainty associated with the non-homogeneity of the profile (especially the random distribution of rock pinnacles, boulders, cavities and zones of various consistencies), which could not be determined in sufficient detail to support a comprehensive 3D analysis of each viaduct pier foundation, a simplified approach for back-calculating stiffness moduli was necessary.

A single stiffness value was calculated at each monitoring point by calculating the average stress increase below each point using the Boussinesq vertical stress distribution and dividing that by the average strain at that point. The average strain was calculated by dividing the monitoring point settlement by the average thickness of compressible materials above bedrock at that pier location as determined from the site investigation data. This analysis resulted in the following approximations.

- It disregarded the 3D non-homogeneity of the soil profile, as this could not be captured in detail by the ground investigation.
- It assumed the bedrock profile to be flat at each pier position.
- It ignored contributions from lateral stress effects (Poisson effects).
- It ignored the fact that Boussinesq stress distribution applies to a semi-infinite homogeneous half-space rather than a profile of limited depth.
- It disregarded yielding of the soil.

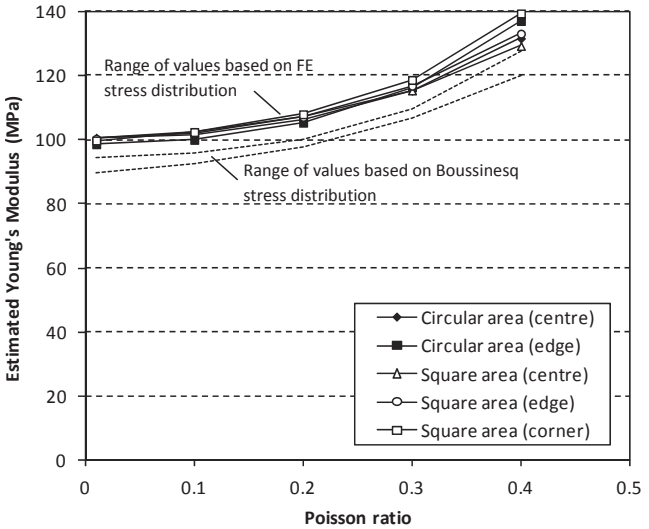

Fig. 5. Average profile stiffness as a function of Poisson ratio based on vertical stress distribution from finite element (FE) analysis.

- It assumed a uniform soil stiffness with depth.
- It neglected the fact that owing to the geometry of the kentledge, and inter-block friction, the loading may not be considered as fully flexible.

Performance of the simplified back-calculation method in a homogeneous soil

The method for the back-calculation of the average profile stiffness was tested by applying it to the settlement and stress distribution calculated from an axi-symmetrical linear-elastic finite element model and a similar 3D model of a square footing. In the models, the stiffness (Young's modulus) of a homogeneous 30 m deep profile was set to a value of 100 MPa. A flexible surcharge of 200 kPa was applied at the surface and the corresponding settlement under the load was calculated.

The vertical stress increase with depth under the centre and edge of the surcharge were calculated from the finite element analyses, as well as using the Boussinesq formulae, and the average stress increase was determined. The average stress increase was divided by the average strain to obtain an average profile stiffness modulus. This was repeated for Poisson ratios between 0.01 and 0.4.

The back-calculated stiffnesses as functions of the Poisson ratio are displayed in Figure 5. Figure 5 is based on the average vertical stress increase determined from the finite element analyses, but also indicates the range of stiffness values should the Boussinesq stress distributions be used.

The back-calculated stiffness is correct for Poisson ratios tending to zero and becomes increasingly an overestimate as the Poisson ratio increases. For Poisson ratios between 0.2 and 0.3, a likely range for many unsaturated or drained soils, the overestimate is *c*. 10–15%. The method is less suitable for soils with high Poisson ratios such as saturated clays or when undrained loading is applicable.

When stiffnesses are back-calculated from the Boussinesq stress distributions, the correct estimates of profile stiffness occur at a Poisson ratio of *c*. 0.2 for the geometry analysed. However, Figure 5 shows that average profile stiffness values back-calculated using a Boussinesq stress distribution are still reasonable.

Given the many other uncertainties associated with a dolomitic profile, the approximate method for back-calculating stiffness was considered acceptable and was subsequently used for the back-calculation of stiffness values from the surcharge trials.

Observed settlements

As a typical example, Figure 6 presents the settlement recorded at Pier 26, plotted over time during the stacking of the surcharge blocks, as well as the rebound during their removal. Levelling point 1 was damaged and data for this point are therefore not available. Settlements increased with placement of every layer of blocks after which it remained approximately constant, except for a small amount of additional settlement, probably attributable to creep. The time taken to place the surcharge varied from site to site, but generally took between 8 and 14 days to complete. It was generally found that settlements stabilized within 1 week to 10 days of completion of the surcharge in chert-dominated profiles. Up to 40 mm of collapse settlement was observed at the corners and along the sides of the surcharge at two pier positions underlain by loose transported sands after significant rainfall. When the surcharge was removed, some rebound took place, but leaving significant permanent deformation.

Applied pressure versus displacement graphs for the loading and unloading cycles, monitored at the various positions on Pier 26, are presented in Figure 7. Settlements generally increased approximately linearly with applied pressure at the centre and mid-passage positions, but the settlement rate reduced with increasing pressure along the mid-sides and especially the corners.

A histogram showing the distribution of settlement recorded at Pier 26 is presented in Figure 8, together with a plan showing the monitoring point locations. The observed settlements are compared with expected theoretical distributions in the discussion. Figure 9a presents the average settlement at the corners, centre, mid-side and mid-passage positions of all piers, and Figure 9b shows settlements normalized by the average settlement for that particular pier. Observed settlement varied considerably, both on single pier positions and between pier positions. Figure 9 indicates that the largest settlements generally occurred at the corners, followed by the mid-side positions, whereas the centres and mid-passage positions generally settled by similar amounts. It also shows that the settlements are almost all within ±50% of the mean measured values, which can be considered relatively uniform when the extreme variation in ground geometry (Fig. 1) and material properties (Table 1) are considered.

As the largest settlements generally occurred at the corners of the surcharge, the survey team interpreted this as being the result of the slight overhang of the blocks (see Fig. 3) and considered these readings to be unrealistic. Corner readings were subsequently not recorded at all surcharge trials.

Back-calculated profile stiffness values

Stiffness values were back-calculated from settlements using the approach described above. Reflecting the observed settlements, the back-calculated stiffnesses varied considerably on single pier positions and also between piers. The distribution of back-calculated stiffnesses at Pier 26 is presented in Figure 10, which also shows the monitoring point locations to which they apply. Figure 11a presents the average stiffness at the corners, centre, mid-side and mid-passage positions of all surcharged piers, and Figure 11b shows stiffness values normalized by the average stiffness calculated at each particular pier. The lowest stiffnesses were calculated at the corners, followed by the mid-side positions, and the stiffnesses at the centres and mid-passage positions were the highest.

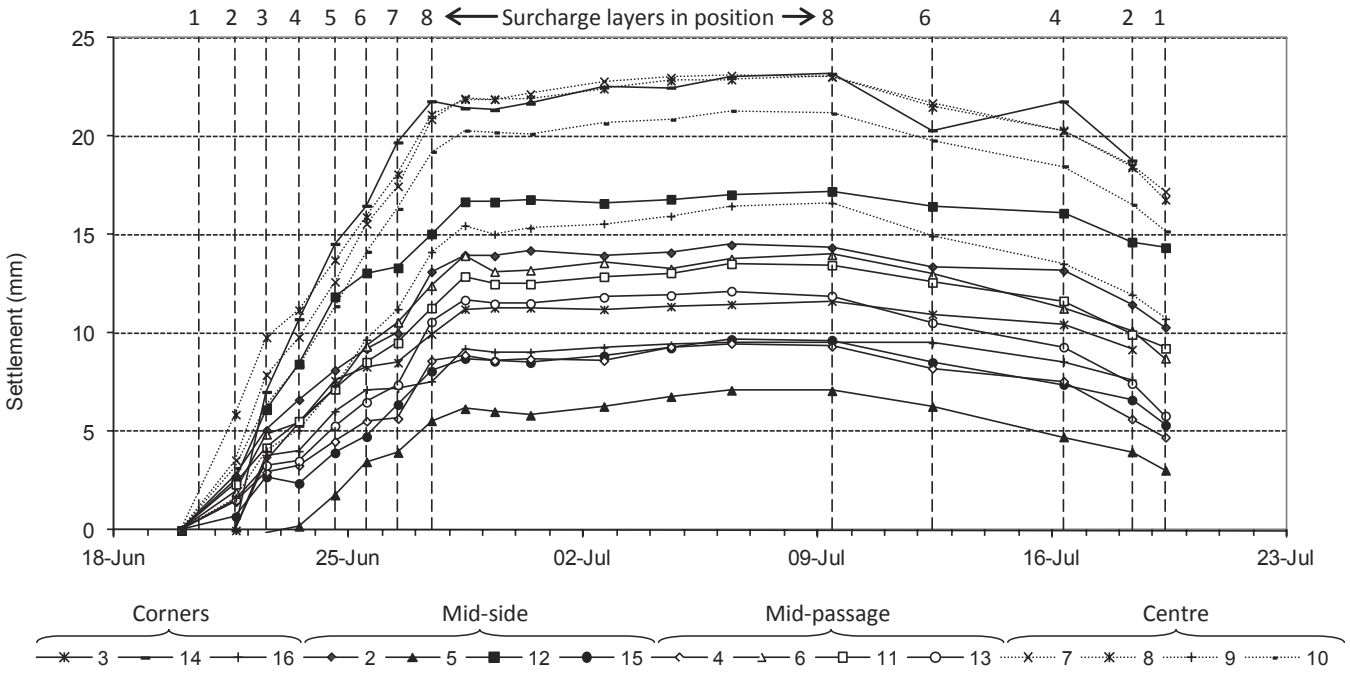

Fig. 6. Movement of first layer of blocks during placement and removal of surcharge load at Pier 26.

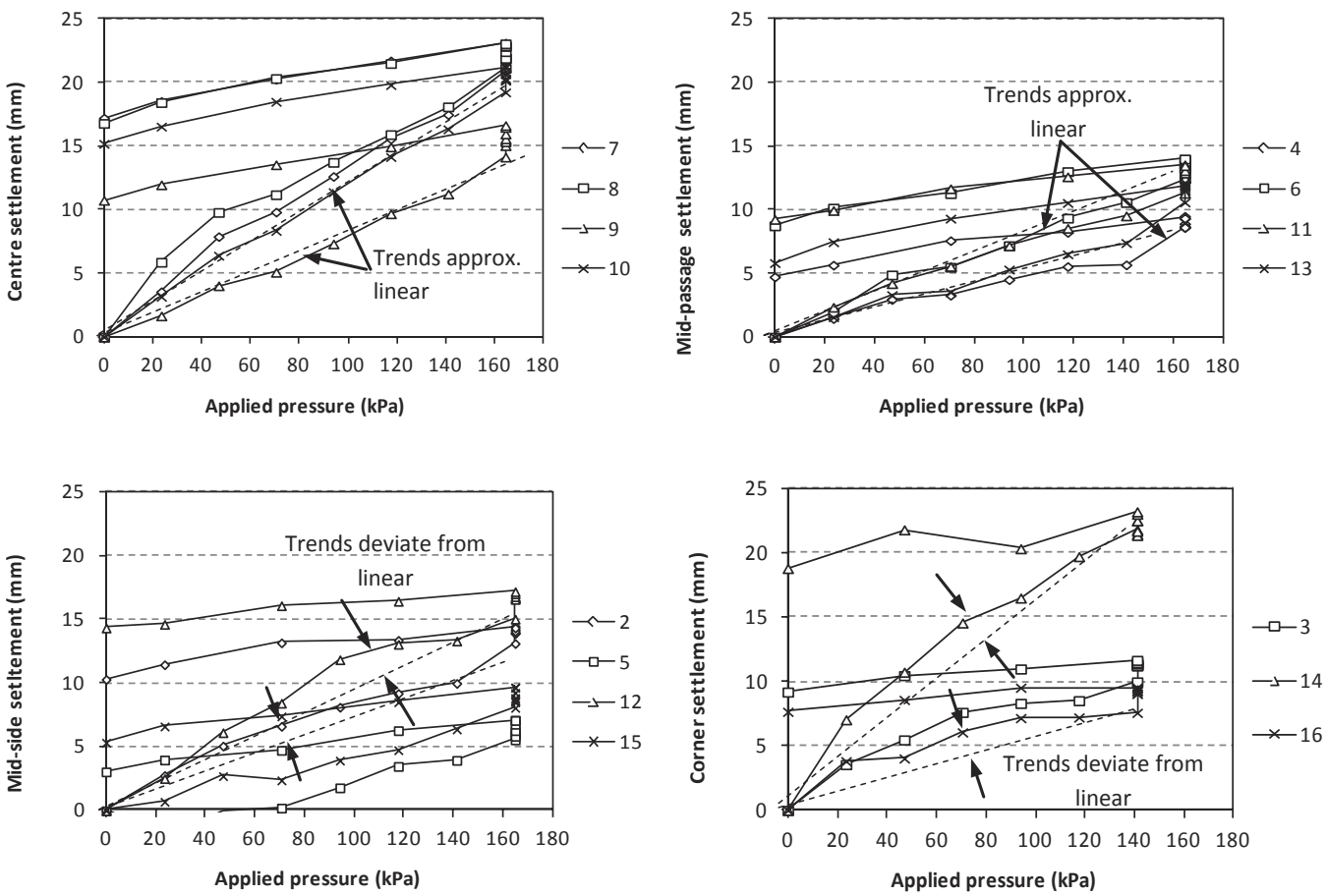

Fig. 7. Applied pressure versus settlement on first layer of blocks observed at the mid-sides, mid-passage, centre and corners of Pier 26.

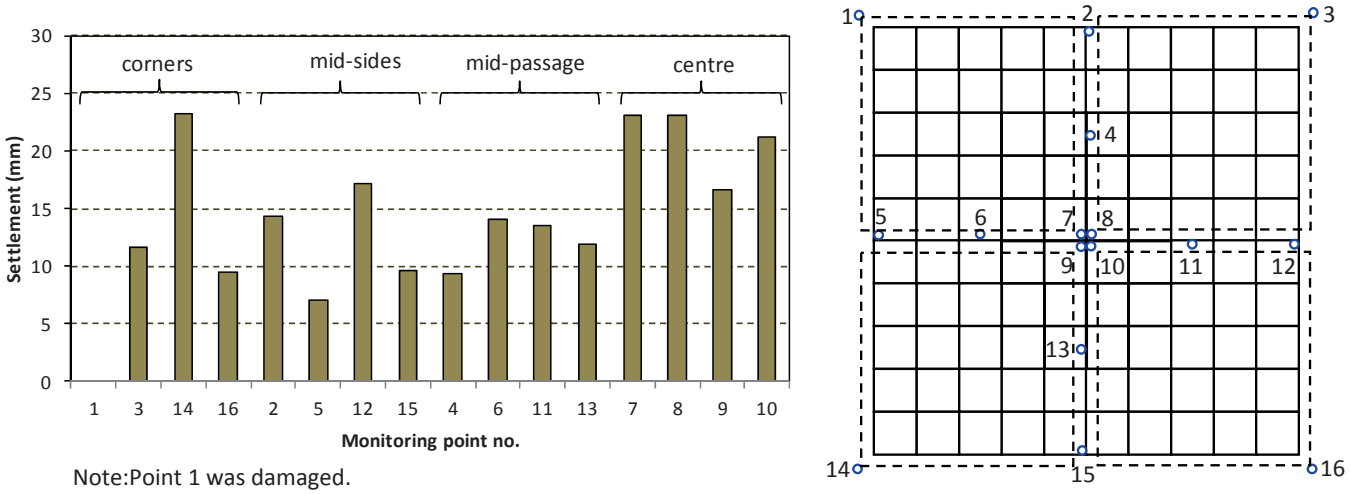

Fig. 8. Distribution of maximum measured settlement on the first layer of blocks at Pier 26.

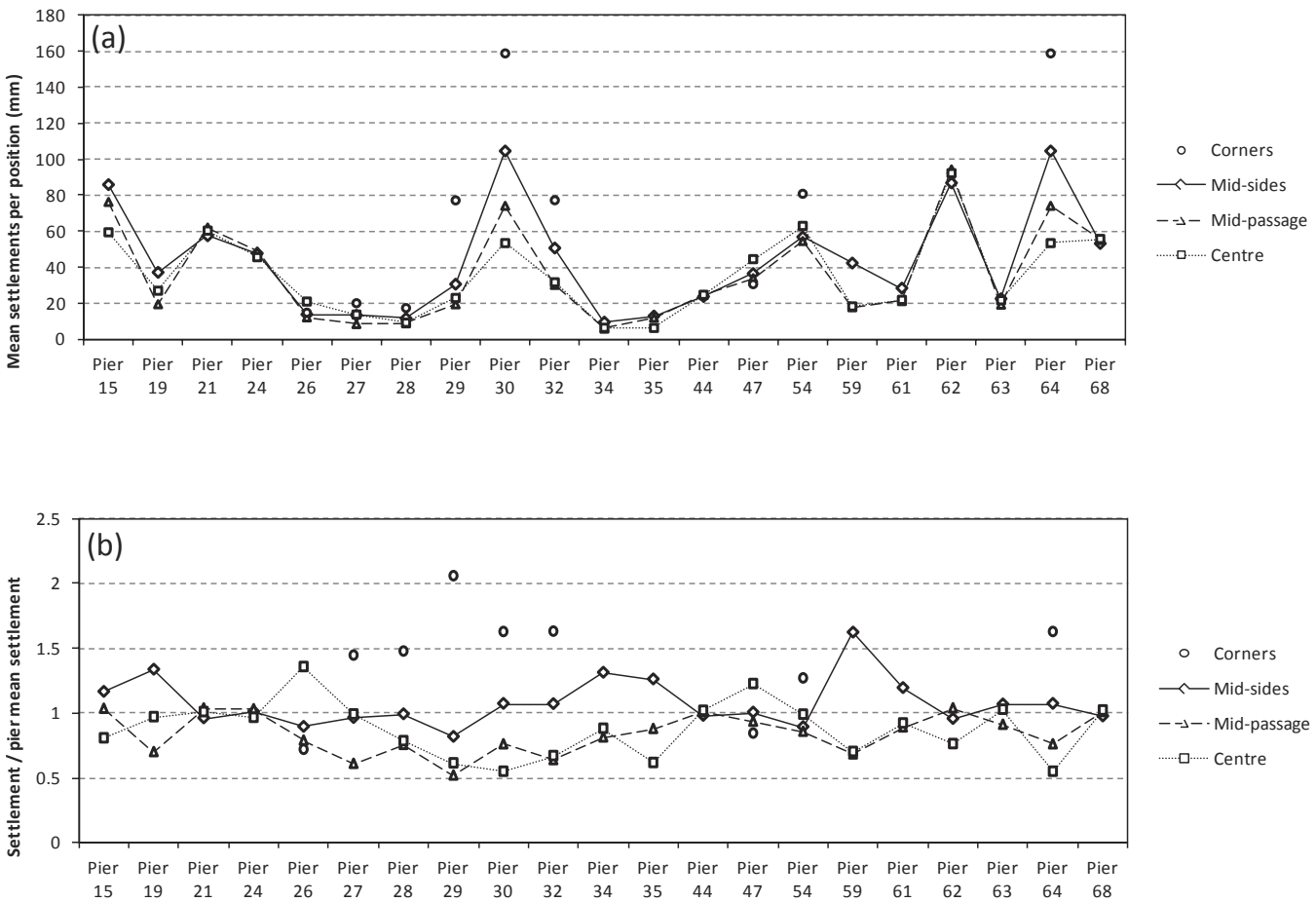

Fig. 9. Actual and normalized settlement of the first layer of blocks at mid-side, mid-passage, centre and corner positions of surcharged piers along the viaduct.

The stiffness data are tabulated in Table 2, presenting the minimum and maximum values per pier, as well as the average values and standard deviations. A log-normal distribution was found to describe the stiffness data relatively well.

Figure 12 illustrates the variation in minimum, average and maximum Young's moduli back-calculated at the various piers graphically and also the variation in average depth to bedrock at each pier. Also shown are typical Young's moduli from plate load tests on chert gravel and wad from Wagener (1982). By plotting average settlement and stiffness against profile depth (Fig. 13a and b), a very weak correlation between the thickness of the compressible soil layer and settlement becomes evident, but virtually no correlation with the back-calculated stiffness is evident.

Rebound stiffnesses

As illustrated in Figure 6, some rebound took place upon removal of the surcharge. This was considerably less than the settlement that occurred, reflecting the increase in stiffness

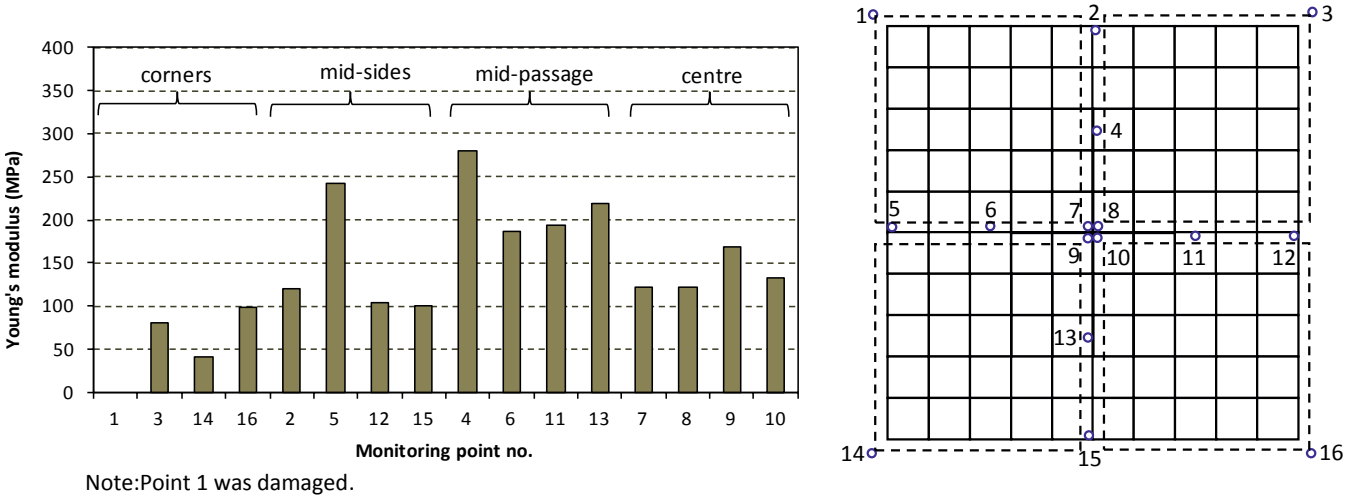

Fig. 10. Distribution of calculated stiffness at Pier 26.

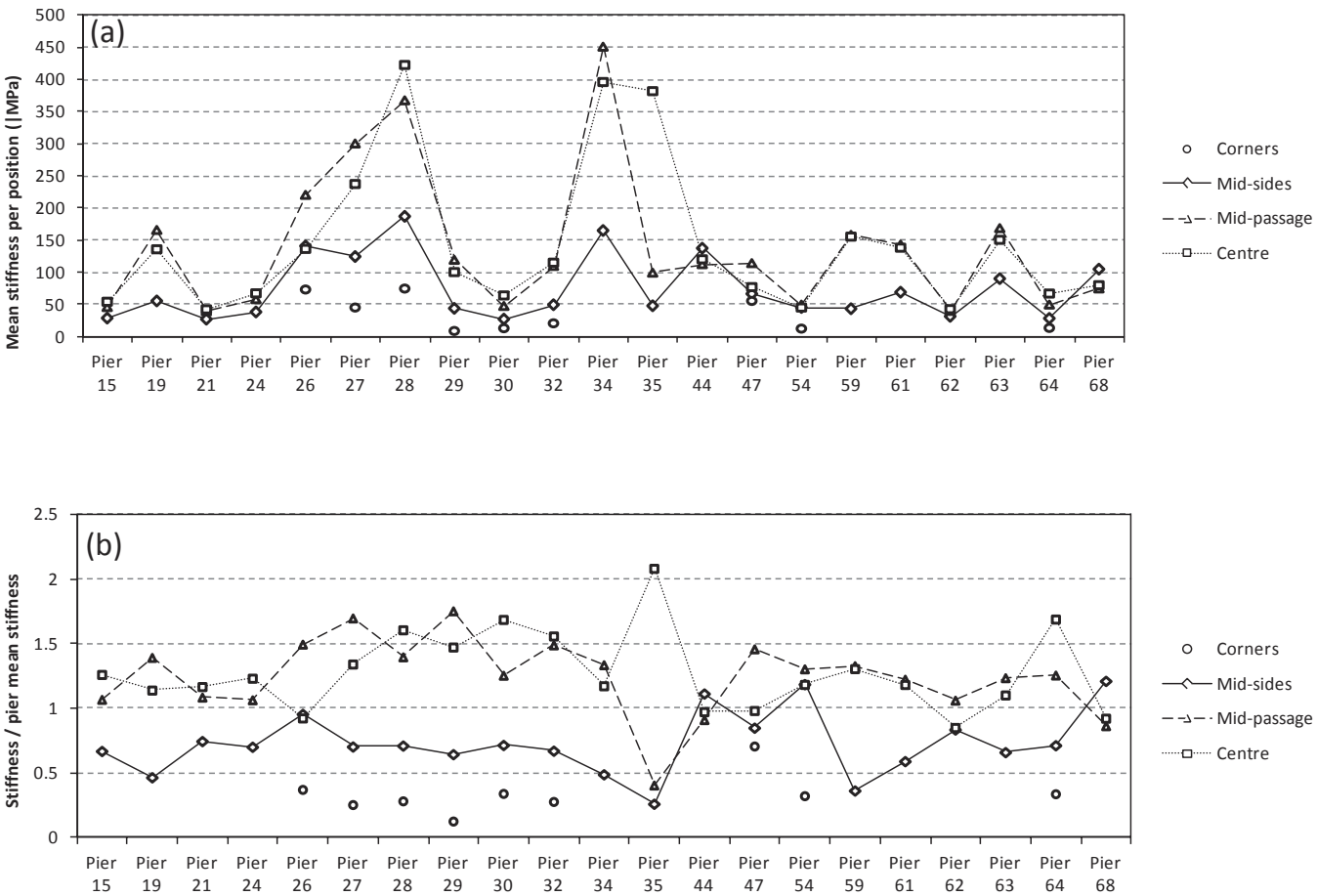

Fig. 11. Normalized stiffness values at mid-side, mid-passage, centre and corner positions of surcharged piers along the viaduct.

owing to the preloading of the soil. Figure 14 presents the ratio of the average rebound stiffness to the average virgin stiffness for the test locations for which rebound data are available. Excluding the three highest values, which are thought to be outliers, the mean rebound stiffness amounted to 3.3 times the virgin stiffness. The outliers are attributable to very small amounts of rebound measured, rather than unusually large virgin settlements.

Discussion

Back-calculated profile stiffness values

Soil stiffness values for foundation design on the dolomites in South Africa have often been determined from plate load tests on the various materials forming the profile. Given the state of knowledge at the time, this approach was reasonable. For example, Ward

Table 2. *Young's moduli back-calculated from surcharge trials*

Pier	Number of points	Young's modulus (MPa)			Standard deviation (σ)	Coefficient of variation (σ/μ)
		Minumum	Average (μ)	Maximum		
1. Pier 15	12	14.5	42.9	81.4	20.2	0.472
2. Pier 19	12	37.5	119.0	266.2	73.2	0.615
3. Pier 21	12	21.1	36.3	47.7	8.9	0.244
4. Pier 24	12	27.3	54.5	88.2	16.9	0.310
5. Pier 26	15	40.4	147.3	280.2	65.9	0.448
6. Pier 27	16	39.6	176.8	445.7	119.8	0.678
7. Pier 28	16	49.5	262.8	534.7	162.6	0.619
8. Pier 29	16	6.0	68.0	149.6	50.3	0.739
9. Pier 30	16	3.7	37.9	105.5	28.4	0.750
10. Pier 32	16	11.2	73.7	151.7	44.3	0.600
11. Pier 34	12	132.6	337.2	729.9	166.4	0.494
12. Pier 35	11	30.4	183.3	725.7	228.7	1.248
13. Pier 44	12	43.9	123.4	384.1	93.3	0.757
14. Pier 47	16	25.2	78.3	170.3	41.8	0.535
15. Pier 54	16	5.5	38.1	74.4	22.7	0.596
16. Pier 59	12	26.4	118.9	202.0	61.7	0.519
17. Pier 61	12	53.9	116.7	204.4	47.0	0.402
18. Pier 62	11	21.9	37.6	47.6	8.7	0.230
19. Pier 63	12	69.1	136.4	281.3	58.5	0.429
20. Pier 64	16	3.8	39.6	110.3	29.8	0.752
21. Pier 68	12	22.0	86.5	238.7	58.5	0.677
Overall mean		32.6	110.2	253.3	67.0	0.577
Overall standard deviation		28.9	79.2	204.2	57.9	0.222
Overall σ/μ		0.886	0.719	0.806	0.864	0.385

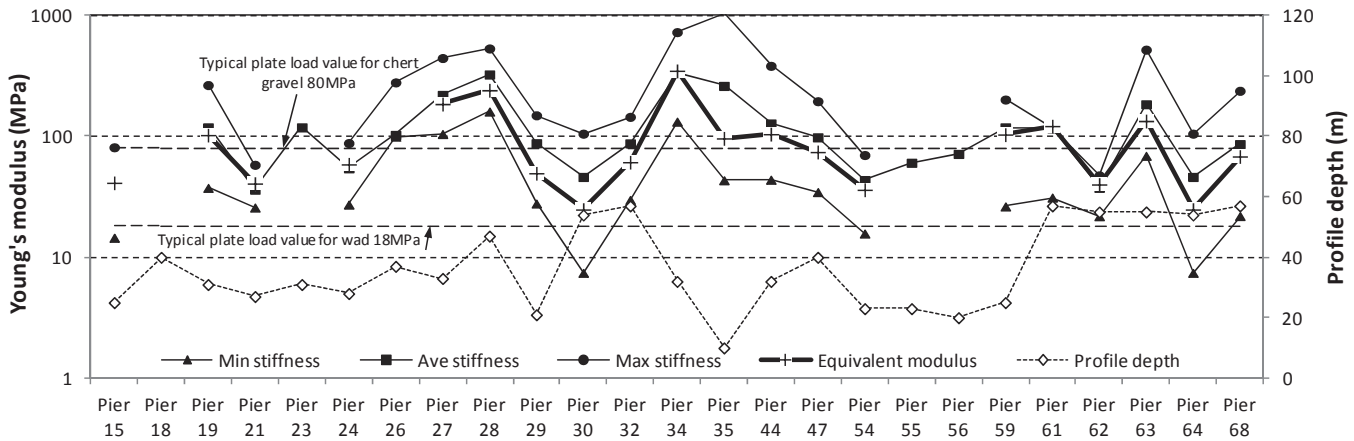

Fig. 12. Average profile stiffness and depth to bedrock along viaduct alignment, also showing typical plate load moduli for wad and chert gravels from Wagener (1982).

et al. (1968) reported agreement between stiffness moduli from a large-scale surcharge trial and plate load tests. Comparing the stiffness values of various dolomitic residuum materials from the literature (Table 1) with those back-calculated from the surcharge trials (Table 2), the mass stiffness of the profile was generally significantly higher than that of its components. This provided justification for the use of higher stiffness values in the design of the Gautrain viaduct than would previously have been used in the absence of large-scale surcharge trial data.

Equivalent stiffness moduli for each surcharge trial were calculated using the average settlement over the entire surcharge area, the average applied stress, and assuming a flexible surcharge load over a finite profile depth. A Poisson ratio of 0.3 was assumed, whereas no Poisson ratio was used in the stiffness calculations first presented. The equivalent moduli are plotted in Figure 12. These values are slightly lower than the average stiffness moduli determined using the simplified method but generally correspond well. Deviations occur because, for many of the surcharge trials, corner settlement values are not available. (The corners usually settled more, significantly affecting the mean settlement values.)

Theoretical versus observed settlement patterns

A typical set of parameters, representative of some surcharge trials, is as follows: loaded area 20 m × 20 m; surcharge pressure 200 kPa; average Young's modulus 100 MPa; estimated Poisson ratio 0.3; depth to bedrock 30 m.

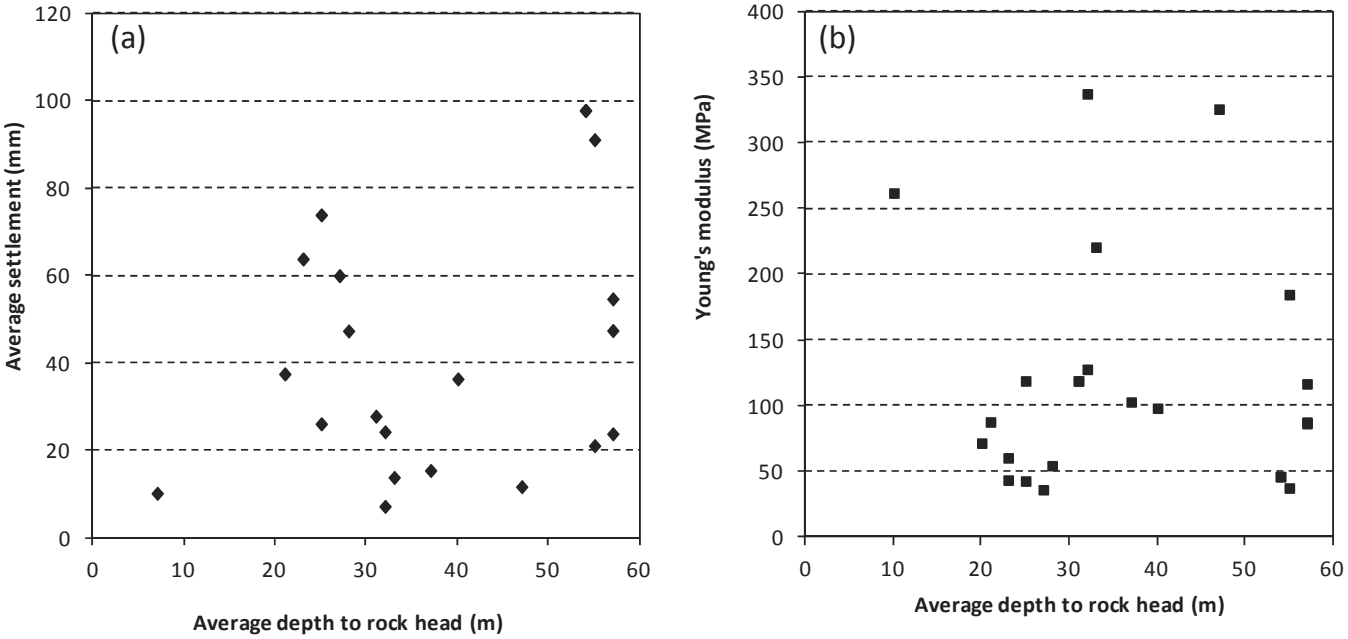

Fig. 13. Average settlement and Young's modulus versus depth to rock.

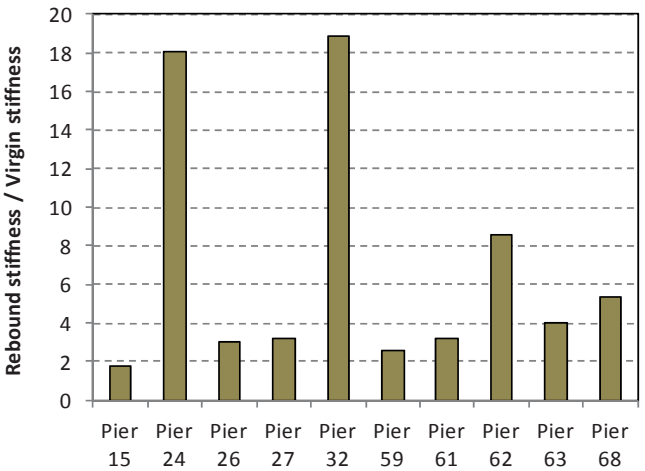

Fig. 14. Ratio of rebound stiffness to virgin stiffness for piers with reload data available.

The settlements required to be observed at the various monitoring point locations to produce a stiffness value of 100 MPa in the situation above are presented in Figure 15. The variability in settlement is a consequence of the variation in contact stress under the applied load; for example, for a flexible surcharge the contact stress under a corner is only one-quarter of the value at the centre. The correlation between settlement and stiffness therefore varies depending on the monitoring location. This illustrates why there appears to be no or poor correlation between settlement and calculated stiffness when comparing Figure 8 and Figure 10, the data from Pier 26.

An elastic settlement calculation (see, e.g. Poulos & Davis 1974) based on these parameters, assuming stiffness homogeneity and isotropy, predicts the maximum settlement to occur at the centre, with mid-side positions settling by 60% of the maximum and the corners by 37% of the maximum. Elastic settlements decrease smoothly from the centre towards the outside and a considerable amount of settlement is predicted to occur relatively far outside the loaded area (see, e.g. Gibson 1967).

On a non-homogeneous profile with linearly increasing stiffness with depth, the settlement pattern is much more localized around the loaded area and the surcharge itself is expected to undergo less differential settlement than in the aforementioned case (see Gibson 1967). This was also physically observed around a large surcharge trial by Ward et al. (1968). A localization of strain and deformation around the loading boundaries can also be modelled by taking into account the non-linear stress–strain behaviour of soils (Jardine et al. 1986). Non-linear behaviour results from non-linear soil stiffness and yielding. However, Jardine et al. (1986) reported that non-linear stiffness affects settlement well before first yielding.

Depending on the stiffness gradient with depth, stiffness anisotropy and compressibility (i.e. the Poisson ratio), Rodrigues (1975) has shown that the maximum settlement of a flexible surcharge would not necessarily occur under the centre, but that it could occur nearer to the edges when stiffness increases with depth and when the horizontal Young's modulus exceeds the vertical (see, e.g. also Simons & Menzies 2001).

Owing to the scatter in observed settlements from the surcharge trials, a relatively coherent settlement pattern becomes apparent only when the all the normalized settlement data are studied as a whole. Figure 9b shows that the maximum settlement tended to occur at the corners, followed by the mid-side positions and then the mid-passage and centre positions, which underwent settlements of similar magnitude. This observation suggests that soil stiffness increased with depth and possibly that the horizontal soil stiffness exceeded the vertical. A stiffness increase with depth is also suggested by the fact that settlements were localized around the surcharge as mentioned above. Although it is likely that the stiffness in the residual dolomite profile increases for some distance below the surface, it is known that it reduces again in the compressible wad material occurring above and in the gullies between the bedrock pinnacles.

The observed settlement pattern also raises a question regarding the actual flexibility or rigidity of the surcharge stacks. A perfectly flexible surcharge is expected to be resisted by an uniform-in-plan subgrade reaction, whereas, as rigidity of the loaded area is increased, elevated stresses are expected near the perimeter of the loaded area compared with those near the centre (see Boswell & Scott 1975). This raises the question of whether the larger settlements along the

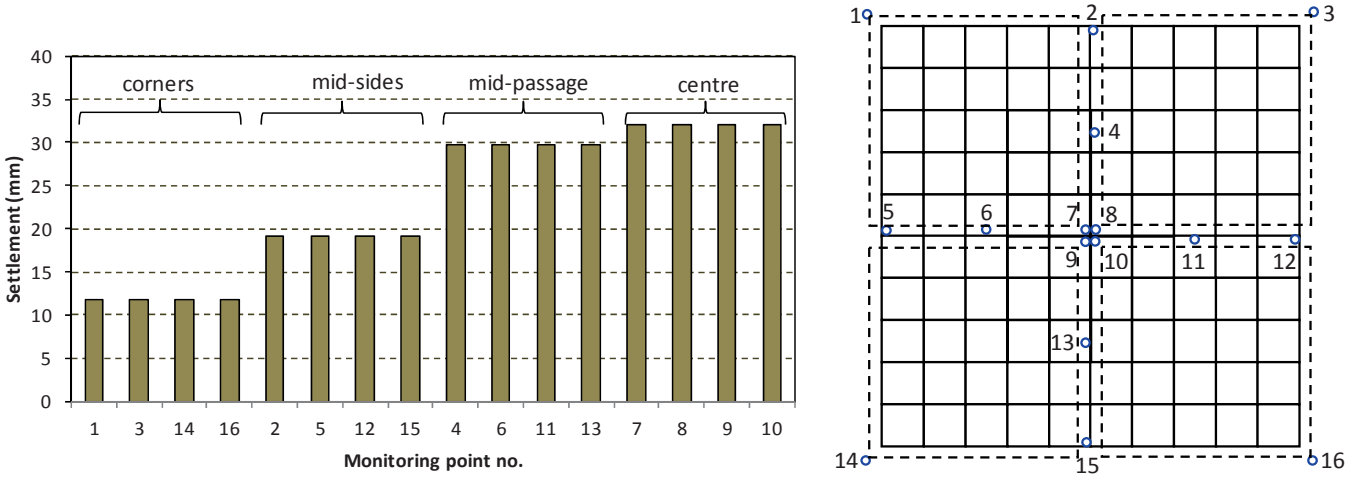

Fig. 15. Distribution of settlements resulting in a back-calculated stiffness of 100 MPa.

edges could perhaps be a consequence of higher stresses being exerted there because of the rigid behaviour of the surcharge stacks. Despite not being structurally connected, the configuration of blocks forming the surcharge stacks (see Fig. 3b) would not have been perfectly flexible. The observed settlement pattern therefore appears to be a consequence of both increasing soil stiffness with depth (at least to a certain depth) and the relative rigidity of the surcharge stacks. Doing away with the passage between surcharge quadrants from the third trial onwards would have increased the overall rigidity of the surcharge stack, probably resulting in it behaving more like a rigid foundation.

The above observations have implications for the back-analysis of stiffness values from settlements. The simple method for the back-analysis of stiffness assumed a homogeneous, isotropic, linear elastic subgrade, loaded by a perfectly flexible surcharge. This approach stems from a design office environment where structural engineers requested linear elastic parameters, necessitating that conservative stiffness values had to be determined in a short space of time.

More accurate stiffness may be calculated by assuming the surcharge to possess some rigidity and by taking into account non-homogeneity (increase in stiffness with depth up to a point), as well as stiffness anisotropy and non-linearity (i.e. a modern constitutive soil model). Should this be done, higher stresses at the corners and edges, given the same settlements, will result in higher stiffness values being calculated there, whereas somewhat lower stiffnesses will be calculated near the centre, reducing the scatter in stiffness data presented in Figure 11. A comprehensive analysis would, however, require subsurface settlement data and is outside the scope of this paper.

Variation in back-calculated stiffness values

Reasons for the large variation in settlement data were investigated by excavating a number of test pits (to *c.* 3 m depth) on the footprints of some surcharged areas after removal of the load. Materials encountered varied widely from relatively soft manganese-rich sandy clayey silts, reworked residual syenite, densely packed chert gravels and boulders, and naturally transported materials to fills of various origins and consistencies.

The highest stresses from the surcharge occur immediately below the surcharge but reduce as stresses distribute with depth. As stress is distributed with depth, stiffer zones would tend to support most of the load, as a result of arching, probably leaving most of the compressible zones virtually unloaded. The behaviour of the surcharge is therefore unlikely to be affected much by soft inclusions (e.g. pockets of wad or cavities) at depth within a matrix of stiffer material (chert boulders and gravels). However, at the surface this stress distribution had not yet occurred, so that the presence of near-surface zones of various consistencies is more likely to affect surcharge settlement. This variation in consistency of near-surface materials observed during the test pit investigation is thought to be the main reason for the scatter in stiffness data. The dolomite residuum is extremely heterogeneous.

As alluded to above, the stiffness variation is also to some extent likely to have been a consequence of the method of back-analysis, but the evidence suggests that this is of secondary importance relative to the variability in stiffness of the near-surface materials.

Little or no correlation between stiffness and depth to bedrock was found (Fig. 13).

Designing for differential settlement on dolomite residuum

The highly variable nature of the near-surface material and the observed associated settlement (see Fig. 8) suggest that it appears reasonable and conservative to recommend that differential settlements on similar soil profiles be estimated as equal to the maximum calculated surface settlement. This can be compared against the usual practice to typically design for between one-third and two-thirds of this value, depending on the soil profile (Simons & Menzies 2001).

Conclusions

The design of the Gautrain viaduct through Centurion required stiffness parameters to be determined, representative of the underlying soil profile and the loading imposed by the viaduct. The residual dolomite profile underlying the line is extremely heterogeneous and impossible to characterize in a representative way using routine (e.g. plate load or laboratory) tests. A series of large-scale surcharge trials, designed to exert loads similar to that imposed by the viaduct, was carried out from which representative mass stiffness values could be calculated. The mean stiffness values thus determined corresponded well to equivalent moduli calculated from elastic solutions based on average surcharge settlements.

The settlement data were found to be highly variable. The variability is ascribed to the surcharge being sensitive to the variations in the consistency of the heterogeneous near-surface materials. As stress distributes with depth, stiffer materials would tend to carry most load so that the behaviour of the surcharge would become less sensitive to the presence of compressible pockets at depth. Compressible materials at depth will not be loaded, or will be loaded only lightly.

A secondary contributor to settlement variability results from the mass-behaviour of the surcharge stacks. Despite being able to settle differentially, it appears that the surcharge exerts a load distribution-in-plan similar to a load with rigidity, with the perimeter being more heavily loaded and subsequently settling more than the centre. This is contrary to the initial expectation of a flexible surcharge, but could also be a consequence of non-homogeneity in stiffness with depth or stiffness anisotropy. The surcharge blocks were expected to behave as a flexible load as they were free to move independently. This has implications for the back-calculation of stiffness from the settlement data because the load applied by the surcharge at the surface is not uniform in plan.

Improvements in back-calculating stiffnesses from the settlement data can be made by taking into account non-homogeneity of stiffness with depth and non-linear soil stiffness. Calibration of such models requires settlement data at various depths. The effects of soil yield are considered to be of secondary importance.

The mass stiffness values back-calculated from the results of the surcharge trials were found to be significantly higher than the values quoted in the literature for components of a residual dolomite profile, typically chert gravels and wad (see Fig. 12). Values in the literature are mostly based on plate load test results. This meant that less conservative stiffness moduli could be used in the design of the foundations of the Gautrain viaduct, resulting in a more economical design.

It is recommended that the potential differential foundation settlement be estimated as equal to the total expected settlement.

Acknowledgements. The author wishes to thank the Gauteng Province and Bombela CJV for permission to publish the information contained in this paper. The author also wishes to express his gratitude to C. Clayton for his support in drafting this paper.

References

Bombela CJV 2007. *Assumptions Report, Detail Design 6A, Foundation Design Part 1 of 2*. Bombela CJV, Report **CJV-L05-CDE-2664 0805**.

Boswell, L.F. & Scott, C.R. 1975. A flexible circular plate on a heterogeneous elastic half-space: Influence coefficients for contact stress and settlement. *Géotechnique*, **25**, 604–610.

Buttrick, D.B. 1986. Wad and ferroan soil developed in the dolomitic area south of Pretoria. MSc thesis, University of Pretoria.

Carrier, W.D. & Christian, J.T. 1973. Rigid circular plate resting on a non-homogeneous elastic half-space. *Géotechnique*, **23**, 67–84.

Gibson, R.E. 1967. Some results concerning displacements and stresses in a non-homogeneous elastic half-space. *Géotechnique*, **17**, 58–67.

Gibson, R.E. 1974. The analytical method in soil mechanics. *Géotechnique*, **24**, 115–140.

Jardine, R.J., Potts, D.M., Fourie, A.B. & Burland, J.B. 1986. Studies on the influence of non-linear stress–strain characteristics in soil–structure interaction. *Géotechnique*, **36**, 377–396.

Johnson, M.R., Anhaeusser, C.R. & Thomas, R.J. 2006. *The Geology of South Africa*. Geological Society of South Africa and Council for Geoscience, Pretoria.

Poulos, H.G. & Davis, E.H. 1974. *Elastic Solutions for Soil and Rock Mechanics*. Wiley, New York.

Rodrigues J.S. 1975. *The development and application of a finite element program for the solution of geotechnical problems*. PhD Thesis, University of Surrey, Guildford.

Simons, N.E. & Menzies, B.K. 2001. *A Short Course on Foundation Engineering*, 2nd edn. Thomas Telford, London.

Tosen, R., Storry, R.B. & Hoeben, S. 2009. Borehole radar cavity and discontinuity assessment in dolomite for Gautrain. *In*: *Proceedings of ISRM Regional Symposium, Eurock 2009, Dubrovnik*. Balkema, Rotterdam, 387–392.

Wagener, F. von M. 1982. *Engineering construction on dolomite*. PhD thesis, University of Natal.

Ward, W.H., Burland, J.B. & Gallois, R.W. 1968. Geotechnical assessment of a site at Mundford, Norfolk, for a large proton accelerator. *Géotechnique*, **18**, 399–431.